

# Superconducting Berry Curvature Dipole

Oles Matsyshyn,<sup>1,\*</sup> Giovanni Vignale,<sup>2</sup> and Justin C. W. Song<sup>1,†</sup>

<sup>1</sup>*Division of Physics and Applied Physics, School of Physical and Mathematical Sciences,  
Nanyang Technological University, Singapore 637371*

<sup>2</sup>*The Institute for Functional Intelligent Materials (I-FIM),  
National University of Singapore, 4 Science Drive 2, Singapore 117544*

(Dated: October 30, 2024)

Superconductivity and Bloch band Berry curvature responses represent two distinct paradigms of quantum coherent phenomena. The former relies on the collective motion of a many-body state while the latter proceeds from the momentum-space winding of Bloch wavefunctions. Here we reveal a superconducting Berry curvature dipole (BCD) that arises as a collective many-body phenomena in noncentrosymmetric superconductors. Strikingly, we find the superconducting BCD is sensitive to the *phase* of the superconducting gap and depends on the noncentrosymmetric structure of its pairing. This unusual property enables a BCD proximity effect in hybrid quantum materials that induces nonreciprocity even in a target centrosymmetric metal. We find superconducting BCD naturally produces nonreciprocal electromagnetic responses that includes a giant second-order nonlinearity. This renders noncentrosymmetric superconductors an exciting platform for realizing pronounced nonlinearities and its BCD responses a novel diagnostic of the superconducting gap.

Bloch band quantum geometry plays a surprisingly critical role in electronic nonreciprocity [1–7]: the asymmetry of forward and backward flows [1]. A prime example is the Berry curvature dipole (BCD) [2] that endows electrons with a range of nonreciprocal responses that include nonlinear Hall currents even in the presence of time-reversal symmetry [2, 8, 9], electro-optic modulation and amplification without population inversion [10–12], as well as means for energy harvesting in the terahertz regime [11]. Traditionally viewed as a single-particle property, finite net BCD is often thought to rely on the presence of a Fermi surface in noncentrosymmetric metals. As a result, net BCD vanishes in a band insulator with a gapped quasiparticle spectrum [2, 13]. What is the fate of the BCD when a noncentrosymmetric metal undergoes a superconducting transition so that its Fermi surface is gapped out by electron interactions?

Here we reveal a superconducting Berry curvature dipole (sBCD) in fully gapped noncentrosymmetric superconductors. We find sBCD is a collective phenomena of the entire superconducting state. Unlike single particle BCD in a metal produced when an electric field shifts the electronic distribution function, sBCD arises even as the occupation of Bogoliubov quasiparticles remains fixed in a fully occupied Bogoliubov band. As we argue, sBCD arises due to geometric phases accumulated in the quantum coherent superconducting wavefunction when a supercurrent flows. This many-body effect renders sBCD distinct from that of its parent metallic state persisting even for a gapped spectrum.

We identify two contributions to sBCD: an order parameter BCD that is sensitive to the *phase* of the superconducting gap and a parent BCD that tracks the

BCD of the parent metallic state. Strikingly, order parameter BCD directly depends on the structure of the pairing. It vanishes for centrosymmetric pairing even when the Bloch states of the parent metal are noncentrosymmetric. Instead, order parameter BCD activates for a non-centrosymmetric pairing and persists even when the parent metal Bloch electronic states are *centrosymmetric*. This unconventional behavior means that sBCD can spontaneously develop from a centrosymmetric parent metal state, or be proximitized in a centrosymmetric metal by a noncentrosymmetric superconducting substrate. The latter BCD proximity effect has no analog in non-interacting electrons and vividly displays how broken centrosymmetry in the order parameter is encoded in its many body Berry curvature dipole.

We expect pronounced sBCD arises in a range of noncentrosymmetric superconductors, such as rhombohedral trilayer graphene (RTG) [14]. In these, superconducting BCD can be directly probed through a range of non-dissipative and nonreciprocal electromagnetic responses below the superconducting gap, e.g., a supercurrent induced dynamical Hall conductivity (and corresponding magneto-optical Kerr effect) as well as an sBCD second-order nonlinearity. We find the sBCD second-order nonlinearity is giant outstripping that from nonlinearities in noncentrosymmetric metals by more than three orders of magnitude. Given the phase sensitive order parameter BCD, we anticipate such sBCD induced non-reciprocal responses can be used as a novel phase sensitive diagnostic of the superconducting gap operating in bulk systems.

*Interacting Berry curvature dipole.* We begin by examining the dynamics of an electronic material with electron interactions driven by an electromagnetic field with vector potential  $\mathbf{A}(t)$ . This can be tracked via the set of many body states  $|\Phi(\mathbf{A})\rangle$ . Here and below, we have suppressed explicit time dependence  $t$  for brevity.  $|\Phi(\mathbf{A})\rangle$  forms a manifold of states with a geometrical structure [15]. For instance, the quantum geometric tensor of

\* oles.matsyshyn@ntu.edu.sg

† justinsong@ntu.edu.sg

its tangent vector space can be tracked via  $G^{\alpha\beta}(\mathbf{A}) = i(\hbar^2/e^2)\text{Tr}[P(\partial_{\mathbf{A}}^{\alpha}P)(\partial_{\mathbf{A}}^{\beta}P)]$  where  $P(\mathbf{A}) \equiv |\Phi(\mathbf{A})\rangle\langle\Phi(\mathbf{A})|$  is a projector onto the many body state and  $\partial_{\mathbf{A}}^{\alpha} \equiv \partial/\partial A^{\alpha}$ .  $G^{\alpha\beta}(\mathbf{A})$  plays a critical role in describing the response of quantum matter:  $\text{Re}[\lim_{\mathbf{A}\rightarrow 0} G^{\alpha\beta}(\mathbf{A})]$  captures the quantum metric important for bounds of capacitance [16], superfluidity [17], and optical absorption [18];  $\text{Im}[\lim_{\mathbf{A}\rightarrow 0} G^{\alpha\beta}(\mathbf{A})]$ , on the other hand, is the Berry flux that determines the Hall conductivity [19].

Higher moments of quantum geometry can also be generated. Of special interest is the Berry curvature dipole:

$$\mathcal{D}^{\alpha\beta\gamma} = \frac{i\hbar^3}{e^3} \lim_{\mathbf{A}\rightarrow 0} \text{Tr}[P\partial_{\mathbf{A}}^{\alpha}(\partial_{\mathbf{A}}^{\beta}P)(\partial_{\mathbf{A}}^{\gamma}P)] - (\beta \leftrightarrow \gamma). \quad (1)$$

Taking a metallic  $|\Phi(\mathbf{A})\rangle = \prod_{n,s,\mathbf{k}\leq\mathbf{k}_F} \hat{c}_{\mathbf{k},n,s}^{\dagger}(\mathbf{A})|0\rangle$  produces the BCD in a non-interacting metal as [2, 20]

$$\mathcal{D}_{\text{FS}}^{\alpha\beta\gamma} = \sum_{\{n,\mathbf{k}\}\in o,\{m,\mathbf{k}\}\in\emptyset} i\partial_{\mathbf{k}}^{\alpha}(r_{nm}^{\beta}r_{mn}^{\gamma}) - (\beta \leftrightarrow \gamma), \quad (2)$$

where  $\hat{c}_{\mathbf{k},n,s}^{\dagger}(\mathbf{A})|0\rangle = e^{i\mathbf{k}\cdot\mathbf{r}}|n,\mathbf{k} + \frac{e}{\hbar}\mathbf{A}\rangle$  is the  $s$ -spin,  $n$ -th band creation operator of the Bloch state with periodic part  $|n,\mathbf{k}\rangle$ . Here and below, we have suppressed explicit  $s$  dependence for simplicity so that  $r_{nm}^{\gamma} = \langle n,\mathbf{k}|i\partial_{\mathbf{k}}^{\gamma}|m,\mathbf{k}\rangle$  is the generalized Bloch state Berry connection;  $o/\emptyset$  stand for occupied/unoccupied respectively. Note  $\sum_m \partial_{\mathbf{k}}^{\alpha}(r_{nm}^{\beta}r_{mn}^{\gamma})$  is the property of a Bloch state  $|n,\mathbf{k}\rangle$  and since it is a full derivative,  $\mathcal{D}_{\text{FS}}^{\alpha\beta\gamma}$  vanishes for fully occupied bands [2]. As a result,  $\mathcal{D}^{\alpha\beta\gamma}$  has been thought to only manifest for finite Fermi surfaces [2, 13].

We now argue the opposite:  $\mathcal{D}^{\alpha\beta\gamma}$  can manifest without a Fermi surface in interacting quantum matter. As a prime illustration, we consider a superconducting state:

$$|\text{SC}(\mathbf{A})\rangle = \prod_{\mathbf{k}} \hat{\alpha}_{-\hbar\mathbf{k},\hbar\mathbf{q}+e\mathbf{A},\uparrow} \hat{\alpha}_{\hbar\mathbf{k},\hbar\mathbf{q}+e\mathbf{A},\downarrow} |0\rangle, \quad (3)$$

where  $\hat{\alpha}$  is the Bogoliubov quasi-particle annihilation operator, composed of electrons and holes. Notice that the product runs over the entire lower Bogoliubov band so that  $|\text{SC}(\mathbf{A})\rangle$  describes a gapped phase. We have included a finite Cooper pair momentum  $\hbar\mathbf{q}$  in Eq. (3) to highlight the way electromagnetic waves couple to the superconducting state. Indeed, unlike a metal where the vector potential couples to individual electron momentum  $\hbar\mathbf{k}$ , in a superconductor the vector potential couples to  $\hbar\mathbf{q}$ . As a result, by applying Eq. (3) to Eq. (1), we obtain a superconducting Berry curvature dipole (sBCD), see Supplementary Information SI, as:

$$\mathcal{D}_{\text{sBCD}}^{\alpha\beta\gamma} = \lim_{\mathbf{q}\rightarrow 0} \sum_{\{a,\mathbf{k}\}\in o,\{b,\mathbf{k}\}\in\emptyset} i\partial_{\mathbf{q}}^{\alpha}(\mathcal{A}_{ab}^{\beta}\mathcal{A}_{ba}^{\gamma}) - (\beta \leftrightarrow \gamma), \quad (4)$$

where  $\mathcal{A}_{ab}^{\gamma} = \langle\psi_a(\mathbf{k},\mathbf{q})|i\partial_{\mathbf{q}}^{\gamma}|\psi_b(\mathbf{k},\mathbf{q})\rangle$  is a  $\mathbf{q}$ -Berry connection of the Bogoliubov wave-function (see below for explicit form) and  $a, b$  indexes the Bogoliubov bands.

Critically,  $\partial_{\mathbf{q}}^{\alpha}(\mathcal{A}_{ab}^{\beta}\mathcal{A}_{ba}^{\gamma})$  in Eq. (4) is *not* a full derivative in  $\mathbf{k}$ . As a result, the sBCD in Eq. (4) does not vanish even for a gapped superconducting state. This can

be traced to the fact that even as the lower Bogoliubov band is fully occupied, a finite vector potential imparts momentum to the entire superconducting state turning on BCD; this contrasts with that of an insulator where a vector potential does not impart a physical momentum. As we now explain, this coherent motion of the superconducting state induces an sBCD of a *collective* nature distinct from its non-interacting metallic counterpart.

*Superconducting gap and order parameter BCD.* What is the origin of sBCD in a superconductor? To elucidate this, we analyze the superconducting state via a Bogoliubov de Gennes (BdG) Hamiltonian  $\hat{H} = \frac{1}{2} \sum_{\mathbf{k}} \Psi_{\mathbf{k},\mathbf{q}}^{\dagger} \hat{H}_{\mathbf{k},\mathbf{q},\mathbf{A}}^{\text{BdG}} \Psi_{\mathbf{k},\mathbf{q}}$  in the Bloch-Nambu basis (see SI)

$$\hat{H}_{\mathbf{k},\mathbf{q},\mathbf{A}}^{\text{BdG}} = \begin{pmatrix} \hat{H}_{\mathbf{k}+\mathbf{q}+\frac{e}{\hbar}\mathbf{A}(t)}^{(0)} & \hat{\Delta} \\ \hat{\Delta}^{\dagger} & -[\hat{H}_{-\mathbf{k}+\mathbf{q}+\frac{e}{\hbar}\mathbf{A}(t)}^{(0)}]^T \end{pmatrix}, \quad (5)$$

where the Bloch Hamiltonian of the parent material is  $H_{\mathbf{k}}^{(0)} = H_0(\mathbf{k}) - \mu\mathbb{1}$  and the pairing operator is  $\hat{\Delta}$ . Here  $\mu$  is the chemical potential and  $H_{\mathbf{k}}^{(0)}|n,\mathbf{k}\rangle = \epsilon_{\mathbf{k}}|n,\mathbf{k}\rangle$ . In contrast, the  $\Psi$  eigenstates of the BdG Hamiltonian in Eq. (5) describe Bogoliubov quasiparticles that comprise the superconducting state  $|\text{SC}(\mathbf{A})\rangle$  via  $\alpha_{\mathbf{k},\mathbf{q},\mathbf{A}}|0\rangle = [e^{i(\mathbf{k}+\mathbf{q})\cdot\mathbf{r}}, 0, 0, e^{i(\mathbf{k}-\mathbf{q})\cdot\mathbf{r}}]|\Psi_{\mathbf{k},\mathbf{q},\mathbf{A}}\rangle$  in Eq. (3).

We note that  $H_{\mathbf{k}}^{(0)}$  can have a multi-band structure. Nevertheless, as we now explain, insight into the contributions to sBCD can be exposed by focussing on a single Bloch band  $n$  that crosses the Fermi level. In this isolated band approximation,  $\Psi$  takes on a simple form for time-reversal symmetric materials:

$$|\Psi_{\mathbf{k},\mathbf{q}}\rangle = \begin{bmatrix} u_{\mathbf{k},\mathbf{q}}|n,\mathbf{k}+\mathbf{q}\rangle \\ v_{\mathbf{k},\mathbf{q}}|n,\mathbf{k}-\mathbf{q}\rangle \end{bmatrix}, \quad (6)$$

where  $u_{\mathbf{k},\mathbf{q}}$  and  $v_{\mathbf{k},\mathbf{q}}$  are coherence factors determined directly by substituting into Eq. (5) producing a gapped BdG spectrum (Fig. 1a), see also SI. In what follows, we will focus on time reversal symmetric but noncentrosymmetric superconducting systems. The form of Eq. (6) allows for a direct evaluation of the sBCD. In particular, plugging Eq. (6) into Eq. (4), we find the superconducting Berry curvature dipole arises from two components: an ‘‘order parameter BCD’’ and a ‘‘parent BCD’’ as

$$\mathcal{D}_{\text{sBCD}}^{\alpha\beta\gamma} = \int_{\mathbf{k}} \underbrace{\left[ L_n^{\gamma}(\mathbf{k},\mathbf{q}) \partial_{\mathbf{q}}^{\alpha} \partial_{\mathbf{q}}^{\beta} |v_{\mathbf{k},\mathbf{q}}|^2 - (\beta \leftrightarrow \gamma) \right]}_{\text{order parameter BCD distribution}} \Big|_{\mathbf{q}\rightarrow 0} + 2 \int_{\mathbf{k}} \underbrace{|v_{\mathbf{k},\mathbf{0}}|^2 \left( \partial_{\mathbf{k}}^{\alpha} \partial_{\mathbf{k}}^{\beta} r_{nn}^{\gamma}(\mathbf{k}) - \partial_{\mathbf{k}}^{\alpha} \partial_{\mathbf{k}}^{\gamma} r_{nn}^{\beta}(\mathbf{k}) \right)}_{\text{parent BCD distribution}}, \quad (7)$$

where  $2|v_{\mathbf{k},\mathbf{q}}|^2 = 1 - \tilde{\epsilon}_{\mathbf{k},\mathbf{q}}/[(\tilde{\epsilon}_{\mathbf{k},\mathbf{q}})^2 + 4|\Delta_{\mathbf{k},\mathbf{q}}|^2]^{1/2}$  with  $\tilde{\epsilon}_{\mathbf{k},\mathbf{q}} = \epsilon_{\mathbf{k}+\mathbf{q}} + \epsilon_{\mathbf{k}-\mathbf{q}}$  and the superconducting gap matrix element  $\Delta_{\mathbf{k},\mathbf{q}} = \langle n,\mathbf{k}+\mathbf{q}|\hat{\Delta}|n,\mathbf{k}-\mathbf{q}\rangle$ . Importantly,  $L_n(\mathbf{k},\mathbf{q})$  is a new emergent length scale that depends on

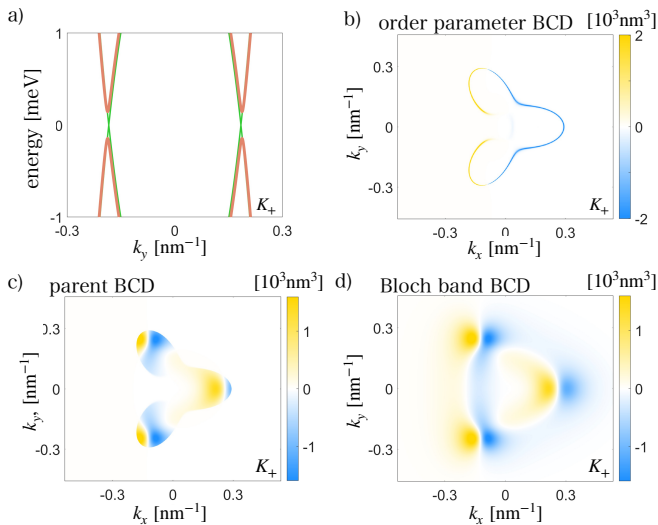


Figure 1. *Berry curvature dipole distribution in a noncentrosymmetric superconductor* **a**. Fully gapped superconducting BdG band structure (red) for gated rhombohedral trilayer graphene (RTG) obtained from a self-consistent numerical solution of Eq.(5). (green) Single-particle electron (and hole) dispersions  $H_{\text{RTG}}^{(0)}(\mathbf{k})$  ( $-H_{\text{RTG}}^{(0)}(-\mathbf{k})$ ) of the parent RTG Fermi surface. **b**. Superconducting order parameter BCD distribution for RTG is peaked close to the BdG band edges and is sensitive to the phase of the gap parameter; distribution obtained by plotting integrand in first term of Eq.(7). **c**. Superconductor Parent BCD distribution mirrors the **d**. single-particle Bloch BCD but is weighted by  $|v_{\mathbf{k},0}|^2$ . Parent BCD is obtained from the integrand of second term in Eq.(7); Bloch state BCD is indicated in the braces. All BCD distributions are shown for the  $K_+$  valley, see full discussion of model parameters in **SI**.

the *phase* of the superconducting gap:

$$\mathbf{L}_n(\mathbf{k}, \mathbf{q}) = -\partial_{\mathbf{q}} \arg \left[ \frac{\langle n, \mathbf{k} + \mathbf{q} | \hat{\Delta} | n, \mathbf{k} - \mathbf{q} \rangle}{\langle n, \mathbf{k} + \mathbf{q} | n, \mathbf{k} - \mathbf{q} \rangle} \right]. \quad (8)$$

It captures a gauge invariant real-space displacement induced by the pairing potential.

The first term of Eq. (7) reveals an order parameter BCD that has no analog for simple non-interacting electrons: it depends on the (gradient of the) phase of the superconducting gap, see Eqs. (7) and (8). Importantly, for a centrosymmetric s-wave pairing potential  $\hat{\Delta} = \Delta \mathbb{I}$ , we find  $\mathbf{L}_n(\mathbf{k}, \mathbf{q})$  *vanishes*. In contrast, when the pairing potential is non-centrosymmetric: e.g., when  $\hat{\Delta}$  possesses a noncentrosymmetric orbital order,  $\mathbf{L}_n(\mathbf{k}, \mathbf{q})$  is finite and contributes significantly to the total sBCD, see explicit example below. This exhibits how  $\mathbf{L}_n(\mathbf{k}, \mathbf{q})$  encodes broken centrosymmetry in the superconducting pairing.

We note that order parameter BCD can dominate the total sBCD in noncentrosymmetric superconductors. Its distribution is sharply peaked for  $\mathbf{k}$  close to the band edge of the lower Bogoliubov band (see Fig 1b and form of  $|v_{\mathbf{k},\mathbf{q}}|^2$ ). Indeed, since the electron and hole spectra in Eq. (5) gap each other out at the Fermi surface to form

the Bogoliubov bands (see Fig 1a), the order parameter BCD distribution traces out the Fermi surface. Strikingly, we find that even for inversion symmetric Bloch wavefunctions  $|n, \mathbf{k}\rangle = |n, -\mathbf{k}\rangle$ , inversion breaking in the pairing  $\hat{\Delta}$  still produces an order parameter BCD. As we will see below, this unusual property enables a superconducting *BCD proximity effect*: non-zero sBCD can be proximitized in a target centrosymmetric metal layer by a proximal noncentrosymmetric superconductor.

The second contribution to  $\mathcal{D}_{\text{sBCD}}^{\alpha\beta\gamma}$  is the parent BCD (Fig 1c) that tracks the BCD distribution of the original Bloch states in the parent metal (Fig 1d). Unlike the original Bloch BCD, parent BCD is weighted by the electron density in the superconductor  $|v_{\mathbf{k},0}|^2$  producing a distribution distinct from that of its parent state. Note,  $|v_{\mathbf{k},0}|^2$  contains the information of superconducting coherence length. This weighting factor is critical since even as the superconductor is *gapped* it enables a non-vanishing parent BCD contribution. Note that the sBCD in Eq. (7) reflects a fully occupied lower Bogoliubov band at zero temperature. At finite temperature, however, thermal excitation of Bogoliubov quasiparticles mean that sBCD distribution from the higher Bogoliubov bands will also contribute.

*Nonlinear Bogoliubov dynamics.* The superconducting BCD in Eq. (7) plays a critical role in the intrinsic non-dissipative response of noncentrosymmetric superconductors. To see this, we examine the dynamics of a Bogoliubov quasiparticle concentrating on slowly varying modulations with frequencies smaller than the superconducting gap. To this end, we write  $\mathbf{v}_{\mathbf{k},a}^{\gamma}(\mathbf{q}) = \langle \Psi_{a,\mathbf{k},\mathbf{q}} | \partial_{\mathbf{q}}^{\gamma} \hat{H}_{\mathbf{k},\mathbf{q},0}^{\text{BdG}} | \Psi_{a,\mathbf{k},\mathbf{q}} \rangle$  and find [21]

$$\mathbf{v}_{\mathbf{k},a}(\mathbf{q}) = \hbar^{-1} \partial_{\mathbf{q}} \varepsilon_{\mathbf{k},a}(\mathbf{q}) - \dot{\mathbf{q}} \times [\nabla_{\mathbf{q}} \times \mathcal{A}_{\mathbf{k},aa}(\mathbf{q})], \quad (9)$$

where  $\hat{H}_{\mathbf{k},\mathbf{q},0}^{\text{BdG}} | \Psi_{a,\mathbf{k},\mathbf{q}} \rangle = \varepsilon_{\mathbf{k},a}(\mathbf{q}) | \Psi_{a,\mathbf{k},\mathbf{q}} \rangle$ . Note that Eq. (9) mirrors that for Bloch electrons in metals [19] but with  $\mathbf{q}$  replacing  $\mathbf{k}$ . In sharp contrast to metals, however, the occupation for  $\mathbf{k}$ -states in Eq. (9) is locked in place: all states in the lower Bogoliubov band are occupied. Indeed, when  $\mathbf{q} = 0$ , the total current in the superconductor  $\mathbf{j} = e \int_{\mathbf{k}} \sum_{\{a\} \in \epsilon_0} v_{\mathbf{k},a}$  vanishes.

Instead, current develops when  $\hbar \mathbf{q} \neq 0$ . To expose the dynamical Bogoliubov responses, we focus on a time-varying  $\mathbf{q}(t) = \mathbf{q}_{\text{sc}} + \mathbf{q}_{\text{ac}} \cos(\omega t)$ , where  $\mathbf{q}_{\text{sc}}$  captures a steady-state supercurrent flow and  $\dot{\mathbf{q}}(t)$  describes its oscillation e.g., induced by external ac electromagnetic field,  $\dot{\mathbf{q}}(t) = -e\mathbf{E}(t)/\hbar$ . Here we take  $\omega \ll \Delta$  ensuring adiabatic evolution. Evolving Eq. (9) we obtain

$$\dot{j}^{\gamma}(t) = \dot{j}_0^{\gamma} + \int_{\omega} [\sigma^{(1)}]_{\omega}^{\gamma\beta} E_{\omega}^{\beta} + \int_{\omega_1, \omega - \omega_1} [\sigma^{(2)}]_{\omega, \omega_1}^{\gamma\alpha\beta} E_{\omega_1}^{\alpha} E_{\omega - \omega_1}^{\beta}, \quad (10)$$

where  $\dot{j}_0^{\alpha} = \frac{e}{\hbar} \rho^{\alpha\gamma} q_{\text{sc}}^{\gamma}$  with  $\rho^{\alpha\gamma} = \int_{\mathbf{k}} \partial_{\mathbf{q}}^{\gamma} \partial_{\mathbf{q}}^{\alpha} \varepsilon_{\mathbf{k}}(\mathbf{q})$  is the superfluid weight and  $\int_{\omega} \equiv \int_{-\infty}^{\infty} \exp[-i\omega t] d\omega / 2\pi$ .

While the first term in Eq. (10) describes conventional supercurrent flow, the remaining terms describe a dy-

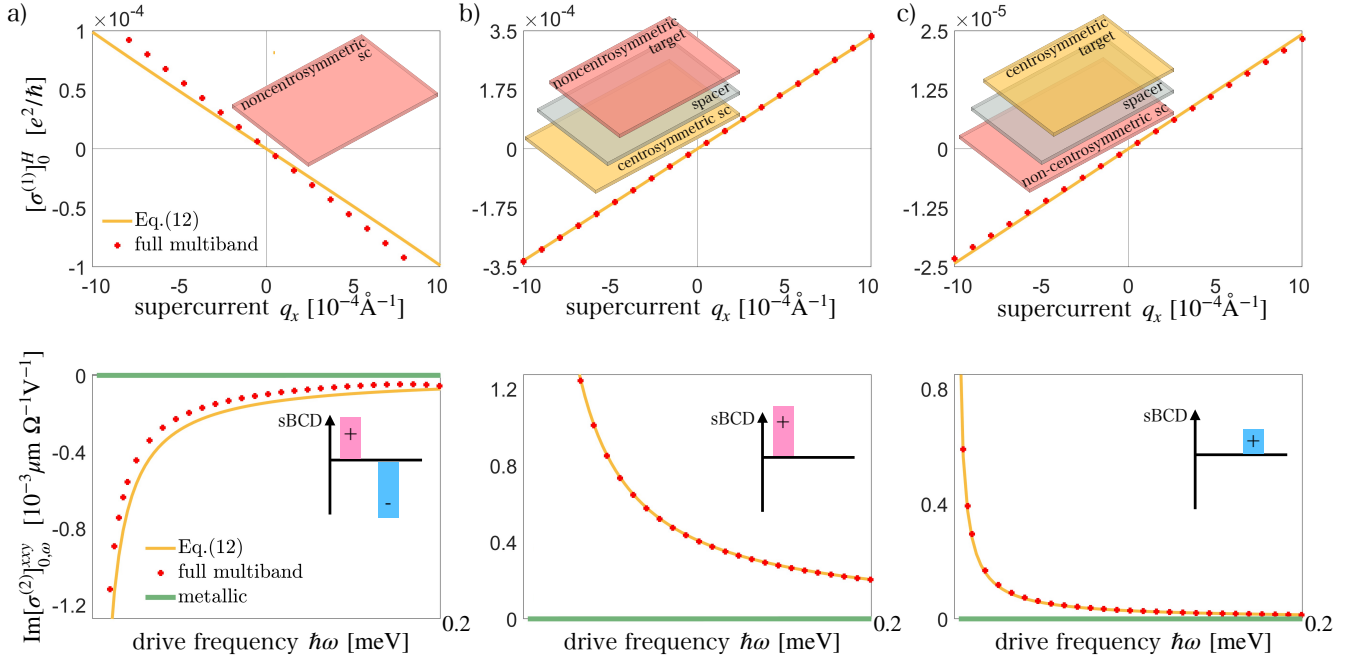


Figure 2. *Superconducting Berry curvature dipole nonreciprocal responses.* Dynamical Hall conductivity as a function of supercurrent (Cooper pair center of mass momentum  $q_x$ ) (top) and second order non-linear conductivity as a function of drive frequency  $\omega$  (bottom) of a target material in three set-ups: **a.** non-centrosymmetric superconductor with a noncentrosymmetric orbital structure for the superconductor pairing  $\hat{\Delta} = [\Delta_A, 0; 0, \Delta_B]$  **b.** non-centrosymmetric target layer with a centrosymmetric proximity induced pairing structure  $\hat{\Delta}_0^{\text{proximity}} = [\Delta_0, 0; 0, \Delta_0]$  **c.** centrosymmetric target layer with a noncentrosymmetric proximity effect: pairing possesses a non-trivial orbital structure  $\hat{\Delta}^{\text{proximity}} = [\Delta_A^{\text{proximity}}, 0; 0, \Delta_B^{\text{proximity}}]$ . Bottom inset illustrates contributions from order parameter (blue) and parent (pink) components to the total sBCD: **a** possess both order parameter and parent BCD, **b** possesses parent BCD while **c** possesses order parameter BCD. To demonstrate the giant sBCD nonlinear response, we compared it against second-order nonlinearities in the parent metal with  $\tau = 1$  ps (green). See **SI** for parameters full discussion of parameters; we have also included a modest strain along the  $x$ -direction (zig-zag) to break rotational symmetry.

namical (linear) conductivity and second-order nonlinearity. Both depend on superconducting Berry curvature dipole. In particular, we find the dynamical Hall conductivity and second-order nonlinearity directly depend on the superconducting BCD:

$$[\sigma^{(1)}]_{\omega}^H = e[\hat{\rho}^{-1} \mathbf{j}_0]^\alpha \mathcal{D}_{\text{sBCD}}^{\alpha\gamma x}, \quad [\sigma^{(2)}]_{\omega, \omega_1}^{\gamma\alpha\beta} = \frac{ie^3}{\hbar^2} \frac{\mathcal{D}_{\text{sBCD}}^{\alpha\beta\gamma}}{\omega_1}, \quad (11)$$

where  $2[\sigma^{(1)}]_{\omega}^H = [\sigma^{(1)}]_{\omega}^{xy} - [\sigma^{(1)}]_{\omega}^{yx}$ . The dynamical Hall conductivity is induced by a steady supercurrent flow while the second order nonlinearity manifests even when  $\mathbf{q}_{\text{sc}} = 0$ . For a monochromatic  $\mathbf{E}(t)$ ,  $[\sigma^{(2)}]_{0,\omega}^{\gamma\alpha\beta}$  produces a rectified photocurrent for circularly polarized irradiation and a second-harmonic generation even for electromagnetic radiation with frequencies below the superconducting gap. This nonlinearity is non-dissipative and is dramatically enhanced in the superconducting state, see below. Notice that  $\mathcal{D}_{\text{sBCD}}^{\alpha\beta\gamma}$  is constrained by point group symmetries. For example, for two-dimensional materials, sBCD has a pseudo-vector nature, and requires all in-plane rotational symmetries (e.g.  $C_{3z}$ ) to be broken [2], see **SI** for symmetry properties of  $\mathcal{D}_{\text{sBCD}}^{\alpha\beta\gamma}$ .

*sBCD in noncentrosymmetric superconducting heterostructures.* We now illustrate sBCD in a two dimensional noncentrosymmetric material. Here we will focus on rhombohedral trilayer graphene (RTG) where centrosymmetry can be readily turned on and off by an external gate. This broken centrosymmetry can be described by an effective bare Hamiltonian for RTG [22, 23]:  $\hat{H}_{\text{RTG}}^{(0)} = \mathbf{d}(\mathbf{k}) \cdot \boldsymbol{\tau} + \delta g(\mathbf{k}) \tau_z$  where  $\boldsymbol{\tau}$  are Pauli matrices describing A/B sublattices,  $\delta$  describes the (external gate-tunable) inversion symmetry breaking and  $\mathbf{d}(\mathbf{p})$  captures the pristine centrosymmetric behavior of RTG when  $\delta = 0$ , see full description of  $\hat{H}_{\text{RTG}}^{(0)}$  and the functional form of  $\mathbf{d}(\mathbf{k}), g(\mathbf{k})$  in **SI**.

Noncentrosymmetric RTG has been observed to host an intrinsic superconducting state [14]. In what follows, we model this by solving the BdG Hamiltonian in Eq. (5) self-consistently with  $\hat{H}^{(0)} = \hat{H}_{\text{RTG}}^{(0)}$ . This produces an order parameter  $\hat{\Delta} = [\Delta_A, 0; 0, \Delta_B]$  that breaks inversion symmetry  $\Delta_A \neq \Delta_B$  [24]. Broken inversion  $\hat{\Delta} = [\Delta_A, 0; 0, \Delta_B]$  have been recently identified as the dominant pairing channel in superconducting RTG [24]. Using this self-consistent solution, we numerically plot



the distribution for the electron-hole and order parameter BCD components of  $\mathcal{D}_{\text{sBCD}}$  in Fig. 1b,c respectively. While parent BCD distribution is diffuse and occurs only for  $\mathbf{k}$  values inside the metallic Fermi surface of RTG, order parameter BCD distribution is sharply peaked along the original RTG parent Fermi surface.

Importantly, in this uniform bulk system, parent and order parameter BCDs are comparable in magnitude but have opposite signs; the net effect of sBCD arises from their competition. To see this, we plot the dynamical Hall conductivity and second-order nonlinearity of Eq. (11) in Fig. 2a (orange lines). The relative contributions of order parameter and parent BCDs are depicted in the lower inset with order parameter outweighing that of parent BCD. The sign of  $\sigma_H^{(1)}$  can be controlled by supercurrent  $q_x$  allowing to tune the corresponding magneto-optical Kerr rotation. Strikingly,  $\sigma^{(2)}$  (orange) obtained from Eq. (11) far exceeds that expected in the RTG metallic state (bright green) by more than three orders of magnitude (at 20 GHz); it continues to rise as  $1/\omega$  providing giant second-order nonlinearities for small  $\omega$ . To check this, we performed a full multiband calculation [25, 26] of the second-order nonlinearity in the superconducting state (red dots) using a quantum Liouville approach, see **SI**. This full treatment reproduces the giant enhancements in second-order nonlinearity when RTG enters the superconducting state with multiband (red dots)  $\sigma_H^{(1)}$  and  $\sigma^{(2)}$  agreeing well with Eq. (11).

To exhibit the importance of the A/B structure of the order parameter in sBCD, we first examine a non-centrosymmetric target metallic layer proximitized by a centrosymmetric superconductor. For simplicity, we use noncentrosymmetric  $\hat{H}_{\text{RTG}}^{(0)}$  in its metallic state as the target layer. Because the superconductor substrate (see schematic inset in Fig. 2b) does not break inversion symmetry, this proximity effect can be modelled with a centrosymmetric pairing  $\hat{\Delta}_0^{\text{proximity}} = [\Delta_0, 0; 0, \Delta_0]$  producing  $\sigma_H^{(1)}$  and  $\sigma^{(2)}$  in Fig. 2b. Importantly, we find order

parameter BCD vanishes (see lower inset). Nevertheless,  $\sigma_H^{(1)}$  and  $\sigma^{(2)}$  persist and are controlled by parent BCD.

For the reverse situation: a centrosymmetric target metallic layer is proximitized by a non-centrosymmetric superconductor. Here we choose  $\hat{H}_{\text{RTG}}^{(0)}$  with  $\delta = 0$  to model the centrosymmetric target layer; due to its centrosymmetry its metallic state should exhibit a zero current induced dynamical Hall conductivity and second-order nonlinearity. Similarly, Bloch state BCD vanishes. However, modeling the proximity effect from the non-centrosymmetric superconductor as  $\hat{\Delta}^{\text{proximity}} = [\Delta_A^{\text{proximity}}, 0; 0, \Delta_B^{\text{proximity}}]$  with  $\Delta_A^{\text{proximity}} \neq \Delta_B^{\text{proximity}}$  produces an order parameter BCD. Even as parent BCD vanishes, the order parameter BCD allows finite  $\sigma_H^{(1)}$  and  $\sigma^{(2)}$  to develop. This demonstrates a type of superconducting BCD proximity effect made possible by the order parameter BCD.

Both parent and order parameter sBCD are *collective* in nature and sharply depart from the familiar BCD for non-interacting electrons. They demonstrate how quantum geometry (and their associated responses) can be dramatically transformed in interacting quantum matter and used to probe the structure of the superconducting gap including its *phase*. Importantly, sBCD produces pronounced non-dissipative responses even for operating frequencies below the superconducting gap. We expect the sBCD  $\sigma_H^{(1)}$  to manifest magneto-optical Kerr effect rotation angles of hundreds of nanoradians within the sensitivity of currently available Kerr effect probes [27]. sBCD  $\sigma^{(2)}$ , on the other hand, is giant outstripping that obtained in good metals by more than three orders of magnitude, rising sharply at low frequencies. This makes noncentrosymmetric superconductors an attractive platform to exploit quantum geometric nonlinearities for superconducting circuits [28].

**Acknowledgements.** We gratefully acknowledge useful conversations with Valla Fatemi, Roshan Krishna Kumar, and Inti Sodemann. This work was supported by Singapore Ministry of Education Tier 2 grant MOE-T2EP50222-0011 (JCWS).

- 
- [1] Yoshinori Tokura and Naoto Nagaosa, “Nonreciprocal responses from non-centrosymmetric quantum materials,” *Nature Communications* **9**, 3740 (2018).
- [2] Inti Sodemann and Liang Fu, “Quantum nonlinear hall effect induced by berry curvature dipole in time-reversal invariant materials,” *Physical review letters* **115**, 216806 (2015).
- [3] Matthew F. Lapa and Taylor L. Hughes, “Semiclassical wave packet dynamics in nonuniform electric fields,” *Phys. Rev. B* **99**, 121111 (2019).
- [4] Arpit Arora, Mark S. Rudner, and Justin C. W. Song, “Quantum plasmonic nonreciprocity in parity-violating magnets,” *Nano Letters* **22**, 9351–9357 (2022).
- [5] Fernando de Juan, Adolfo G. Grushin, Takahiro Morimoto, and Joel E. Moore, “Quantized circular photogalvanic effect in weyl semimetals,” *Nature Communications* **8**, 15995 (2017).
- [6] Junyeong Ahn, Guang-Yu Guo, Naoto Nagaosa, and Ashvin Vishwanath, “Riemannian geometry of resonant optical responses,” *Nature Physics* **18**, 290–295 (2022).
- [7] Takahiro Morimoto and Naoto Nagaosa, “Topological nature of nonlinear optical effects in solids,” *Science Advances* **2**, e1501524 (2016), <https://www.science.org/doi/pdf/10.1126/sciadv.1501524>.
- [8] Qiong Ma, Su-Yang Xu, Huitao Shen, David MacNeill, Valla Fatemi, Tay-Rong Chang, Andrés M Mier Valdivia, Sanfeng Wu, Zongzheng Du, Chuang-Han Hsu, *et al.*, “Observation of the nonlinear hall effect under time-reversal-symmetric conditions,” *Nature* **565**, 337–342 (2019).

- [9] Kaifei Kang, Tingxin Li, Egon Sohn, Jie Shan, and Kin Fai Mak, “Nonlinear anomalous hall effect in few-layer wte2,” *Nature Materials* **18**, 324–328 (2019).
- [10] E. J. König, M. Dzero, A. Levchenko, and D. A. Pesin, “Gyrotropic hall effect in berry-curved materials,” *Phys. Rev. B* **99**, 155404 (2019).
- [11] Li-kun Shi, Oles Matsyshyn, Justin C. W. Song, and Inti Sodemann Villadiego, “Berry-dipole photovoltaic demon and the thermodynamics of photocurrent generation within the optical gap of metals,” *Phys. Rev. B* **107**, 125151 (2023).
- [12] Tatiana G. Rappoport, Tiago A. Morgado, Sylvain Lannebère, and Mário G. Silveirinha, “Engineering transistorlike optical gain in two-dimensional materials with berry curvature dipoles,” *Phys. Rev. Lett.* **130**, 076901 (2023).
- [13] Raffaele Battilomo, Niccolo Scopigno, and Carmine Ortix, “Berry curvature dipole in strained graphene: A fermi surface warping effect,” *Phys. Rev. Lett.* **123**, 196403 (2019).
- [14] Haoxin Zhou, Tian Xie, Takashi Taniguchi, Kenji Watanabe, and Andrea F. Young, “Superconductivity in rhombohedral trilayer graphene,” *Nature* **598**, 434–438 (2021).
- [15] Jonah Herzog-Arbeitman, Valerio Peri, Frank Schindler, Sebastian D. Huber, and B. Andrei Bernevig, “Superfluid weight bounds from symmetry and quantum geometry in flat bands,” *Phys. Rev. Lett.* **128**, 087002 (2022).
- [16] Ilia Komissarov, Tobias Holder, and Raquel Queiroz, “The quantum geometric origin of capacitance in insulators,” *Nature Communications* **15**, 4621 (2024).
- [17] Sebastiano Peotta and Paivi Torma, “Superfluidity in topologically nontrivial flat bands,” *Nature Communications* **6**, 8944 (2015).
- [18] Yugo Onishi and Liang Fu, “Quantum weight,” (2024), [arXiv:2406.06783 \[cond-mat.str-el\]](https://arxiv.org/abs/2406.06783).
- [19] Di Xiao, Ming-Che Chang, and Qian Niu, “Berry phase effects on electronic properties,” *Rev. Mod. Phys.* **82**, 1959–2007 (2010).
- [20] Raffaele Resta, “Theory of longitudinal and transverse nonlinear dc conductivity,” *Phys. Rev. Res.* **4**, 033002 (2022).
- [21] Long Liang, Sebastiano Peotta, Ari Harju, and Päivi Törmä, “Wave-packet dynamics of bogoliubov quasiparticles: Quantum metric effects,” *Physical Review B* **96** (2017), [10.1103/physrevb.96.064511](https://doi.org/10.1103/physrevb.96.064511).
- [22] Fan Zhang, Bhagawan Sahu, Hongki Min, and A. H. MacDonald, “Band structure of abc-stacked graphene trilayers,” *Physical Review B* **82** (2010), [10.1103/physrevb.82.035409](https://doi.org/10.1103/physrevb.82.035409).
- [23] Jeil Jung and Allan H. MacDonald, “Gapped broken symmetry states in abc-stacked trilayer graphene,” *Physical Review B* **88** (2013), [10.1103/physrevb.88.075408](https://doi.org/10.1103/physrevb.88.075408).
- [24] Zhiyu Dong and Leonid Levitov, “Superconductivity in the vicinity of an isospin-polarized state in a cubic dirac band,” (2021), [arXiv:2109.01133 \[cond-mat.supr-con\]](https://arxiv.org/abs/2109.01133).
- [25] Hiroto Tanaka, Hikaru Watanabe, and Youichi Yanase, “Nonlinear optical responses in noncentrosymmetric superconductors,” *Physical Review B* **107** (2023), [10.1103/physrevb.107.024513](https://doi.org/10.1103/physrevb.107.024513).
- [26] Hikaru Watanabe, Akito Daido, and Youichi Yanase, “Nonreciprocal optical response in parity-breaking superconductors,” *Phys. Rev. B* **105**, 024308 (2022).
- [27] Jing Xia, Yoshiteru Maeno, Peter T. Beyersdorf, M. M. Fejer, and Aharon Kapitulnik, “High resolution polar kerr effect measurements of sr<sub>2</sub>ruo<sub>4</sub>: Evidence for broken time-reversal symmetry in the superconducting state,” *Phys. Rev. Lett.* **97**, 167002 (2006).
- [28] Constantin Schrade and Valla Fatemi, “Dissipationless nonlinearity in quantum material josephson diodes,” *Phys. Rev. Appl.* **21**, 064029 (2024).
- [29] Alexander Altland and Ben D. Simons, *Condensed Matter Field Theory*, 2nd ed. (Cambridge University Press, 2010).
- [30] Yiran Zhang, Robert Polski, Alex Thomson, Étienne Lantagne-Hurtubise, Cyprian Lewandowski, Haoxin Zhou, Kenji Watanabe, Takashi Taniguchi, Jason Alicea, and Stevan Nadj-Perge, “Enhanced superconductivity in spin-orbit proximitized bilayer graphene,” *Nature* **613**, 268–273 (2023).
- [31] Stepan S. Tsirkin and Ivo Souza, “On the separation of Hall and Ohmic nonlinear responses,” *SciPost Phys. Core* **5**, 039 (2022).

## Supplementary Information for ‘‘Superconducting Berry Curvature Dipole’’

### Section A: Projectors and Berry curvature dipole in a superconductor

In this section, we demonstrate how to evaluate explicit expressions for the superconducting Berry curvature dipole in the main text. As described in the main text, the projector onto the state of the superconductor is spanned by the set of occupied Bloch Bogoliubov states  $P_{\text{SC}}(\mathbf{A}) = \sum_{a \in o} |\Psi_a(\mathbf{k}, \mathbf{q} + \frac{e}{\hbar} \mathbf{A})\rangle \langle \Psi_a(\mathbf{k}, \mathbf{q} + \frac{e}{\hbar} \mathbf{A})|$ , with vector potential coupled with the Cooper pair center of mass momentum  $\mathbf{q}$ , allowing us to directly compute the Berry curvature dipole of the superconductor as

$$\begin{aligned} \mathcal{D}_{\text{SC}}^{\beta\alpha\gamma} &= \lim_{\mathbf{A} \rightarrow 0} i \frac{\hbar^3}{e^3} \text{Tr}[P_{\text{SC}} \partial_{\mathbf{A}}^{\beta} [(\partial_{\mathbf{A}}^{\alpha} P_{\text{SC}})(\partial_{\mathbf{A}}^{\gamma} P_{\text{SC}})]] - (\alpha \leftrightarrow \gamma) = i \sum_{a \in o} \langle \Psi_a | \partial_{\mathbf{q}}^{\beta} [(\partial_{\mathbf{q}}^{\alpha} P_{\text{SC}})(\partial_{\mathbf{q}}^{\gamma} P_{\text{SC}})] | \Psi_a \rangle - (\alpha \leftrightarrow \gamma) \\ &= \sum_{a \in o, b} \partial_{\mathbf{q}}^{\beta} [\langle \Psi_a | (\partial_{\mathbf{q}}^{\alpha} P_{\text{SC}}) | \Psi_b \rangle \langle \Psi_b | (\partial_{\mathbf{q}}^{\gamma} P_{\text{SC}}) | \Psi_a \rangle] + \\ &\quad \sum_{a \in o, b} \left[ i [\langle \Psi_a | (\partial_{\mathbf{q}}^{\alpha} P_{\text{SC}})(\partial_{\mathbf{q}}^{\gamma} P_{\text{SC}}) | \Psi_b \rangle \mathcal{A}_{ba}^{\beta}] - i [\mathcal{A}_{ab}^{\beta} \langle \Psi_b | (\partial_{\mathbf{q}}^{\alpha} P_{\text{SC}})(\partial_{\mathbf{q}}^{\gamma} P_{\text{SC}}) | \Psi_a \rangle] \right] - (\alpha \leftrightarrow \gamma) \\ &= \sum_{a \in o, b \in \emptyset} i \partial_{\mathbf{q}}^{\beta} (\mathcal{A}_{ab}^{\alpha} \mathcal{A}_{ba}^{\gamma}) - (\alpha \leftrightarrow \gamma), \end{aligned}$$

where we used  $(\partial_{\mathbf{q}}^{\alpha} P_{\text{SC}})(\partial_{\mathbf{q}}^{\gamma} P_{\text{SC}}) = \sum_{abc} \mathcal{A}_{ac}^{\alpha} \mathcal{A}_{cb}^{\gamma} [(\delta_{c \in o} - \delta_{a \in o})(\delta_{c \in o} - \delta_{b \in o})] |a\rangle \langle b|$  in the third line, and relabelled  $a \leftrightarrow b$ , to find that first and second terms cancel. This directly reproduces Eq.(4) of the main text.

The Berry curvature dipole tensor can be expressed as:

$$\mathcal{D}_{\text{sBCD}}^{\alpha\beta\gamma} = \sum_{a \in o, b} i \partial_{\mathbf{q}}^{\alpha} (\mathcal{A}_{ab}^{\beta} \mathcal{A}_{ba}^{\gamma}) - (\beta \leftrightarrow \gamma) = \varepsilon^{\beta\gamma\kappa} i \partial_{\mathbf{q}}^{\alpha} \mathcal{B}^{\kappa} \quad (\text{A-1})$$

with the Levi-Cevita tensor as  $\varepsilon$  and  $\mathcal{B}^{\kappa} = \frac{1}{2} \varepsilon^{\kappa\beta\gamma} \sum_{a \in o, b} \mathcal{A}_{ab}^{\beta} \mathcal{A}_{ba}^{\gamma}$  is a *pseudo-vector*. Note that the sum over  $b$  is unrestricted; this is because the terms  $a \in o, b \in o$  cancel with similar terms in  $(\beta \leftrightarrow \gamma)$ . Note that in addition to broken inversion symmetry, other point group symmetries can also constrain the BCD [2]. In particular, in two-dimensional materials,  $\mathcal{B}^{\kappa}$  has only a  $\mathbf{z}$ -vector component thus finite sBCD requires all in-plane rotational symmetries to be broken for the in plane sBCD to be allowed. As a result, mirror symmetry is the largest point group symmetry compatible with sBCD in a 2D material [2]. For a mirror axis along  $x$ :

$$\mathcal{D}^{xxx} = \mathcal{D}^{xyy} = \mathcal{D}^{yxx} = \mathcal{D}^{yyy} = \mathcal{D}^{yyx} = \mathcal{D}^{xyx} = 0, \quad \mathcal{D}^{xyx} = -\mathcal{D}^{xxxy}. \quad (\text{A-2})$$

### Section B: Bogoliubov de Gennes (BdG) equation and the isolated band approximation

In the following we review the BdG equations starting from a real-space treatment and discuss the isolated band approximation. The BdG equations extend the Bardeen-Cooper-Schrieffer theory to non-homogeneous systems. These are coupled equations for the complex amplitudes  $|u(r)\rangle$  and  $|v(r)\rangle$  in the presence of a finite super-current, where the phase of the gap function becomes a linear function of the center of mass coordinate.:

$$\left\{ \frac{1}{2} [-i\nabla + e\mathbf{A}(\mathbf{r}, \mathbf{t})]^2 \delta_{ss'} + V_{ss'}(\mathbf{r}) - \mu \delta_{ss'} \right\} u_{s'}(\mathbf{r}) + \int d\mathbf{r}' e^{+i\mathbf{q}\cdot(\mathbf{r}+\mathbf{r}')} \Delta_{ss'}(\mathbf{r}, \mathbf{r}') v_{s'}(\mathbf{r}') = E u_s(\mathbf{r}), \quad (\text{B-1})$$

$$- \left\{ \frac{1}{2} [+i\nabla + e\mathbf{A}(\mathbf{r}, \mathbf{t})]^2 \delta_{ss'} + V_{ss'}^*(\mathbf{r}) - \mu \delta_{ss'} \right\} v_{s'}(\mathbf{r}) + \int d\mathbf{r}' e^{-i\mathbf{q}\cdot(\mathbf{r}+\mathbf{r}')} [\Delta_{ss'}(\mathbf{r}, \mathbf{r}')]^{\dagger} u_{s'}(\mathbf{r}') = E v_s(\mathbf{r}). \quad (\text{B-2})$$

An important property of this equation is its *gauge covariance*. Namely if  $|u(r)\rangle$  and  $|v(r)\rangle$  are solutions with potentials  $\hat{V}(\mathbf{r}), \mathbf{A}(\mathbf{r}, \mathbf{t})$ , and  $\hat{\Delta}(\mathbf{r}, \mathbf{r}')$ , then  $|u(r)\rangle \exp[-i\chi(\mathbf{r})]$  and  $|v(r)\rangle \exp[i\chi(\mathbf{r})]$  are solutions with potentials  $V(\mathbf{r}), \mathbf{A}(\mathbf{r}, \mathbf{t}) + \nabla\chi(\mathbf{r})$  and  $\hat{\Delta}(\mathbf{r}, \mathbf{r}') \exp[-i(\chi(\mathbf{r}) + \chi(\mathbf{r}'))]$ . The proof is by direct substitution.

Making use of gauge covariance we see that the solutions with the finite supercurrent will be of the form:

$$|u(\mathbf{r})\rangle = |u_{\mathbf{k}, \mathbf{q}}\rangle e^{i(\mathbf{k}+\mathbf{q})\cdot\mathbf{r}}, \quad |v(\mathbf{r})\rangle = |v_{\mathbf{k}, \mathbf{q}}\rangle e^{i(\mathbf{k}-\mathbf{q})\cdot\mathbf{r}}. \quad (\text{B-3})$$

By introducing the  $\mathbf{k}$ -dependent Hamiltonian as  $H_{\sigma\sigma'}(\mathbf{r}, -i\nabla + \hbar\mathbf{k} + e\mathbf{A}(\mathbf{r}, t)) = e^{-i\mathbf{k}\cdot\mathbf{r}} H_{\sigma\sigma'}(\mathbf{r}, -i\nabla + e\mathbf{A}(\mathbf{r}, t)) e^{i\mathbf{k}\cdot\mathbf{r}}$ , and focusing on uniform vector potentials we write  $\hat{H}_{\mathbf{k}+\frac{e}{\hbar}\mathbf{A}(t)}^{(0)} = e^{-i\mathbf{k}\cdot\mathbf{r}} \hat{H}_0(\mathbf{r}, -i\nabla + e\mathbf{A}(t)) e^{i\mathbf{k}\cdot\mathbf{r}}$ . Applying Eq. (B-3) and the above into Eq.(B-1) we find the familiar  $\mathbf{k}$ -space BdG equations:

$$\hat{H}_{\mathbf{k}+\mathbf{q}+\frac{e}{\hbar}\mathbf{A}(t)}^{(0)} |u_{\mathbf{k},\mathbf{q}}\rangle + \hat{\Delta}_{\mathbf{k},\mathbf{q}} |v_{\mathbf{k},\mathbf{q}}\rangle = E |u_{\mathbf{k},\mathbf{q}}\rangle, \quad (\text{B-4})$$

$$-[\hat{H}_{-\mathbf{k}+\mathbf{q}+\frac{e}{\hbar}\mathbf{A}(t)}^{(0)}]^* |v_{\mathbf{k},\mathbf{q}}\rangle + \hat{\Delta}_{\mathbf{k},\mathbf{q}}^\dagger |u_{\mathbf{k},\mathbf{q}}\rangle = E |v_{\mathbf{k},\mathbf{q}}\rangle \quad (\text{B-5})$$

where  $\hat{\Delta}_{\mathbf{k},\mathbf{q}} = \int d\mathbf{r}' \hat{\Delta}(\mathbf{r}, \mathbf{r}') e^{i\mathbf{k}\cdot(\mathbf{r}'-\mathbf{r})}$  and note,  $[H_{\mathbf{k}}^{(0)}]^* = [H_{\mathbf{k}}^{(0)}]^T$ . For local pairing  $\hat{\Delta}(\mathbf{r}, \mathbf{r}') = \hat{\Delta}\delta(\mathbf{r} - \mathbf{r}')$ , we write  $\hat{\Delta}_{\mathbf{k},\mathbf{q}} = \hat{\Delta}$  producing the simple form Eq.(5) of the main text.

For simplicity we consider a system with no spin orbit coupling  $H_{\mathbf{k},\uparrow}^{(0)} = H_{\mathbf{k},\downarrow}^{(0)}$ . Due to the structure of the BdG equations as in Eqs.(B-4-B-5), and the fact that both  $|m, \mathbf{k} + \mathbf{q}\rangle$  and  $|m, -\mathbf{k} + \mathbf{q}\rangle^*$  form a full basis at every  $\mathbf{k}$ , it is convenient to expand the  $|u_{\mathbf{k},\mathbf{q}}\rangle$  in  $|m, \mathbf{k} + \mathbf{q}\rangle$  basis while  $|v_{\mathbf{k},\mathbf{q}}\rangle$  in  $|m, -\mathbf{k} + \mathbf{q}\rangle^*$ . The solution of the BdG equations can be thus simplified by using the *isolated band approximation* as:

$$|u_{\mathbf{k},\mathbf{q}}\rangle = u_{\mathbf{k},\mathbf{q}} |n, \mathbf{k} + \mathbf{q}\rangle, \quad |v_{\mathbf{k},\mathbf{q}}\rangle = v_{\mathbf{k},\mathbf{q}} |n, -\mathbf{k} + \mathbf{q}\rangle^*, \quad (\text{B-6})$$

leading to the following, simplified (reduced), BdG equations:

$$\begin{pmatrix} \epsilon_{\mathbf{k}+\mathbf{q}} & \Delta(\mathbf{k}, \mathbf{q}) \\ \Delta^*(\mathbf{k}, \mathbf{q}) & -\epsilon_{-\mathbf{k}+\mathbf{q}} \end{pmatrix} \begin{pmatrix} u_{\mathbf{k},\mathbf{q}} \\ v_{\mathbf{k},\mathbf{q}} \end{pmatrix} = \epsilon_{\mathbf{k}}(\mathbf{q}) \begin{pmatrix} u_{\mathbf{k},\mathbf{q}} \\ v_{\mathbf{k},\mathbf{q}} \end{pmatrix}, \quad (\text{B-7})$$

where  $\Delta(\mathbf{k}, \mathbf{q}) = \langle n, \mathbf{k} + \mathbf{q} | \hat{\Delta} | n, -\mathbf{k} + \mathbf{q} \rangle^* = |\Delta(\mathbf{k}, \mathbf{q})| e^{i\arg[\Delta(\mathbf{k}, \mathbf{q})]}$ . For the TRS systems, the isolated band approximation reduces to Eq.(6) of the main text [21].

### Section C: sBCD in the isolated band approximation

In this section, we provide further details of how to obtain Eq.(7) of the main text from the isolated band approximation (IBA) ansatz in Eq.(6) of the main text. The sBCD of Bogoliubov bands can be computed as:

$$\mathcal{D}_{\text{sBCD}}^{\alpha\beta\gamma} = \sum_{a \in \mathcal{O}} \partial_{\mathbf{q}}^\alpha \{ \partial_{\mathbf{q}}^\beta \langle \Psi_a | i\partial_{\mathbf{q}}^\gamma \Psi_a \rangle - \partial_{\mathbf{q}}^\gamma \langle \Psi_a | i\partial_{\mathbf{q}}^\beta \Psi_a \rangle \}, \quad (\text{C-1})$$

where  $a$  is the index of the occupied Bogoliubov band. In case of the IBA, in  $T \rightarrow 0$ , set  $a$  consists of the lower Bogoliubov band.

By solving the Eq.(B-7), we can determine lower and upper Bogoliubov states as  $|\Psi_b\rangle = (u, v)^T$ ,  $|\Psi_a\rangle = (-v^*, u^*)^T$  with  $2\epsilon_{\mathbf{k}}(\mathbf{q}) = \epsilon_{\mathbf{k}+\mathbf{q}} - \epsilon_{\mathbf{k}-\mathbf{q}} \pm E_{\mathbf{k}}(\mathbf{q})$  and:

$$u_{\mathbf{k},\mathbf{q}} = \frac{e^{i\arg[\Delta(\mathbf{k}, \mathbf{q})]/2}}{\sqrt{2}} \sqrt{1 + \frac{\tilde{\epsilon}_{\mathbf{k},\mathbf{q}}}{E_{\mathbf{k}}(\mathbf{q})}}, \quad v_{\mathbf{k},\mathbf{q}} = \frac{e^{-i\arg[\Delta(\mathbf{k}, \mathbf{q})]/2}}{\sqrt{2}} \sqrt{1 - \frac{\tilde{\epsilon}_{\mathbf{k},\mathbf{q}}}{E_{\mathbf{k}}(\mathbf{q})}}, \quad E_{\mathbf{k}}(\mathbf{q}) = \sqrt{4|\Delta(\mathbf{k}, \mathbf{q})|^2 + \tilde{\epsilon}_{\mathbf{k},\mathbf{q}}^2}. \quad (\text{C-2})$$

In order to directly evaluate the sBCD of the lower Bogoliubov band, we first write the superconducting Berry connection as:

$$\begin{aligned} \mathcal{A}_{aa}^\gamma &= \left( -v_{\mathbf{k},\mathbf{q}} \langle n, \mathbf{k} + \mathbf{q} | u_{\mathbf{k},\mathbf{q}} \langle n, \mathbf{k} + \mathbf{q} | \right) i \frac{\partial}{\partial \mathbf{q}^\gamma} \begin{pmatrix} -v_{\mathbf{k},\mathbf{q}}^* |n, \mathbf{k} + \mathbf{q}\rangle \\ u_{\mathbf{k},\mathbf{q}}^* |n, \mathbf{k} - \mathbf{q}\rangle \end{pmatrix} = \\ &= \frac{\tilde{\epsilon}_{\mathbf{k},\mathbf{q}}}{2E_{\mathbf{k}}(\mathbf{q})} \left( \partial_{\mathbf{q}}^\gamma \arg[\Delta(\mathbf{k}, \mathbf{q})] - \langle n, \mathbf{k} + \mathbf{q} | i\partial_{\mathbf{k}}^\gamma |n, \mathbf{k} + \mathbf{q}\rangle - \langle n, \mathbf{k} - \mathbf{q} | i\partial_{\mathbf{k}}^\gamma |n, \mathbf{k} - \mathbf{q}\rangle \right) \\ &\quad + \frac{1}{2} \left( \langle n, \mathbf{k} + \mathbf{q} | i\partial_{\mathbf{k}}^\gamma |n, \mathbf{k} + \mathbf{q}\rangle - \langle n, \mathbf{k} - \mathbf{q} | i\partial_{\mathbf{k}}^\gamma |n, \mathbf{k} - \mathbf{q}\rangle \right). \quad (\text{C-3}) \end{aligned}$$

Next we act with  $\partial_{\mathbf{q}}^\beta$  on Eq.(C-3), considering antisymmetric part of the result in  $(\alpha, \beta)$ , and differentiate again with respect to  $\partial_{\mathbf{q}}^\alpha$  to determine sBCD according to Eq.(C-1). This produces Eq.(7) of the main text.



## Section D: Rhombohedral trilayer graphene with strain

For the results shown in Fig. 2 of the main text, we focus on a strained rhombohedral trilayer graphene [23]:

$$H_{\text{ABC}} = \begin{pmatrix} u_1 + \delta_1 & \frac{1}{2}\gamma_2 & v_0\pi^\dagger & v_4\pi^\dagger & v_3\pi + \gamma_N & v_6\pi \\ \frac{1}{2}\gamma_2 & u_3 + \delta_1 & v_6\pi^\dagger & v_3\pi^\dagger & v_4\pi & v_0\pi \\ v_0\pi & v_6\pi & u_1 & \gamma_1 & v_4\pi^\dagger & v_5\pi^\dagger \\ v_4\pi & v_3\pi & \gamma_1 & u_2 & v_0\pi^\dagger & v_4\pi^\dagger \\ v_3\pi^\dagger + \gamma_N^* & v_4\pi^\dagger & v_4\pi & v_0\pi & u_2 & \gamma_1 \\ v_6\pi^\dagger & v_0\pi^\dagger & v_5\pi & v_4\pi & \gamma_1 & u_3 \end{pmatrix} \text{ in } \begin{bmatrix} A_1 \\ B_3 \\ B_1 \\ A_2 \\ B_2 \\ A_3 \end{bmatrix} \quad (\text{D-1})$$

with  $\pi_\xi = \xi k_x + i k_y$  where  $\xi = \pm 1$  is the valley index and the strain modifies  $(A_1, B_2)$  elements according to Ref.[23]. Parameters will be listed shortly. Similarly to Ref.[22] we set  $v_5 = v_6 = 0$  and assume quantities  $v_0\pi, u_1, u_2, v_3, v_4, \gamma_N$  are small.

For computational simplicity, in our work we will focus on an effective low-energy two band Hamiltonian obtained in a Löwdin decomposition of the six-band hamiltonian in Eq. (D-1). Gathering the leading contributions we find the effective two-band Hamiltonian in  $(|A_1\rangle, |B_3\rangle)$  basis [22, 23] as:

$$\hat{H}_{\text{RTG}}^{(0)}(\mathbf{k}, \xi) = \frac{v_0^3}{\gamma_1^2} \begin{pmatrix} 0 & (\pi_\xi^\dagger)^3 \\ (\pi_\xi)^3 & 0 \end{pmatrix} - \frac{v_0}{\gamma_1} \begin{pmatrix} 0 & \gamma_N \pi_\xi^\dagger \\ \gamma_N^* \pi_\xi & 0 \end{pmatrix} + \delta_2 \left( 1 - 3 \frac{k^2 v_0^2}{\gamma_1^2} \right) \tau_0 + \delta \left( 1 - \frac{k^2 v_0^2}{\gamma_1^2} \right) \tau_z \\ + \left( \delta_1 - \frac{2v_4 v_0 k^2}{\gamma_1} \right) \tau_0 + \left( \frac{1}{2} \gamma_2 - \frac{2k^2 v_0 v_3}{\gamma_1} \right) \tau_x, \quad (\text{D-2})$$

with crystal momentum  $k = |\mathbf{k}|$ ,  $\gamma_N(\mathbf{k}) = \gamma_{N0} e^{-\hbar v_0 k / \gamma_1}$ , with  $\gamma_1 / \hbar v_0 = 0.0573 \text{\AA}^{-1}$  and  $v_i = \sqrt{3} a \gamma_i / (2\hbar)$ ,  $a = 2.46 \text{\AA}$ ,  $\delta = (u_1 - u_3)/2$ ,  $3\delta_2 = (u_1 + u_3)/2 - u_2$ . In the main text we used the notation  $g(\mathbf{k}) = 1 - k^2 v_0^2 / \gamma_1^2$  and  $\mathbf{d}(\mathbf{k}) \cdot \boldsymbol{\tau} \equiv d_0(\mathbf{k})\tau_0 + d_x(\mathbf{k})\tau_x + d_y(\mathbf{k})\tau_y + d_z(\mathbf{k})\tau_z$ . The derived Hamiltonian preserves the time-reversal symmetry, while  $\delta$  can be controlled by external gate potential breaks inversion symmetry and the strain  $\gamma_N^*$  breaks  $C_{3z}$  [23]. Parameters are adopted from Refs.[22, 23] in eV as:

$\gamma_0$	$\gamma_1$	$\gamma_2$	$\gamma_3$	$\gamma_4$	$\delta$	$\delta_1$	$\delta_2$	$\gamma_{N0}$
3.1	0.38	-0.015	0.29	0.141	0.06	-0.0105	-0.0023	0.02

## Section E: Bogoliubov de Gennes equations, self consistency, and model parameters

We adopt the standard mean field Bogoliubov de Gennes description of a superconductor with a local attractive density-density interaction potential  $\hat{V}_{\text{el-el}}^{s\bar{s}'}(\mathbf{r} - \mathbf{r}') = -U\delta(\mathbf{r} - \mathbf{r}')\delta_{s,\bar{s}'}$ , where  $s, \bar{s}$  are the opposite spins, due to the Pauli blocking. The supercurrent is introduced by modelling the order parameter with a real space dependence as  $\Delta(\mathbf{r}) = \Delta e^{2i\mathbf{q}\cdot\mathbf{r}}$ . We employ local in space constant pairing Ref.[24], where the pairing occurs between the electrons of opposite momenta ( $\mathbf{k}$  of  $K_+$  valley with  $-\mathbf{k}$  of  $K_-$  valley). Note our treatment is agnostic to the mechanism for attraction; nevertheless we note that in RTG, attraction between electrons has been proposed to originate from soft critical fluctuations near isospin-polarized states in rhombohedral trilayer graphene [24].

We account for the effect of electron-electron interactions in the self-consistent Hartree-Fock fashion by self-consistently solving  $\Delta_{\mathbf{q},ab} = -U \sum_{\mathbf{k}} \langle c_{-\mathbf{k}+\mathbf{q},a} c_{\mathbf{k}+\mathbf{q},b} \rangle$ , which is equivalent to a Free energy minimization. Writing the Greens function of the BdG system as  $\mathcal{G}_{\mathbf{k},\mathbf{q},\omega_n}^{\text{BdG}} = [i\omega_n - \hat{H}_{\mathbf{k},\mathbf{q},0}^{\text{BdG}}]^{-1}$  [29], with Fermionic Matsubara frequency  $\hbar\omega_n = \pi\beta^{-1}(2n+1)$ , the Free energy reads as:

$$F_{\mathbf{q}} = \frac{\Delta_0^2}{2U} - \frac{1}{2\beta} \sum_{k,n} \text{Tr} \ln [\mathcal{G}_{\mathbf{k},\mathbf{q},\omega_n}^{\text{BdG},-1}] \Rightarrow \frac{\partial F(\Delta_A, \Delta_B)}{\partial \Delta_i} = 0 \Rightarrow \frac{\Delta_i}{U} = \frac{1}{2} \sum_k \text{Tr} \{ f(\hat{H}_{\mathbf{k},\mathbf{q},0}^{\text{BdG}}) \partial_{\Delta_i} \hat{H}_{\mathbf{k},\mathbf{q},0}^{\text{BdG}} \}, \quad (\text{E-1})$$

where we used  $\partial_x \ln[A^{-1}(x)] = A(x) \partial_x A^{-1}(x)$  and  $\sum_n \frac{1}{i\hbar\omega_n - E_a} = f(E_a)$ . Note, for the effective model described in the previous section, summation over  $\mathbf{k}$  in the self-consistent scheme above includes summation over both valleys leading to a single global  $\hat{\Delta}$ . Consequently, we write the mean-field Bogoliubov-de-Gennes (BdG) Hamiltonian for each valley as:

$$\hat{H}_{\mathbf{k},\mathbf{q},0}^{\text{BdG}}(\xi) = \begin{pmatrix} \hat{H}_{\text{RTG}}^{(0)}(\mathbf{p} + \mathbf{q}, \xi) - \mu\tau_0 & \hat{\Delta} \\ \hat{\Delta}^\dagger & -\hat{H}_{\text{RTG}}^{*(0)}(-\mathbf{p} + \mathbf{q}, -\xi) + \mu\tau_0 \end{pmatrix}. \quad (\text{E-2})$$

In order to study the the superconducting BCD, we examined superconducting RTG. We adopted  $\mu \approx 17$  meV (point of high DoS)  $\delta = 0.06$  meV and a cut-off frequency of  $\hbar\omega_D = 40$  meV for the self-consistent treatment. For illustration we used  $U = 60$ meV yielding a modest  $T_c \approx 1$  K. We note, parenthetically,  $T_c$  in graphene stacks can be controlled e.g., in hybrid graphene stack layered with a transition metal dichalcogenides [30]. Self consistently determined order parameter at  $T = 0$  K is  $\Delta_A \approx 1.5 \cdot 10^{-1}$  meV,  $\Delta_B \approx 10^{-2}$ meV. We find the gap opening in the spectrum of the BdG Hamiltonian of order  $\Delta_{\text{SC}} \approx 2 \cdot 10^{-1}$  meV. As a result, in Fig.2a we used  $\Delta \approx [0.15, 0; 0, 0.01]$  meV,  $\delta = 0.06$  meV,  $\mu \approx 17$  meV.

To illustrate the proximity effect from a centrosymmetric superconducting on noncentrosymmetric RTG in Fig.2b we chose  $\hat{\Delta} \approx [0.15, 0; 0, 0.15]$  meV,  $\delta = 0.06$  meV,  $\mu \approx 17$  meV. Similarly, to illustrate the proximity effect of a noncentrosymmetric superconductor in centrosymmetric target layer (in this case RTG) in Fig.2c we adopted  $\hat{\Delta} \approx [0.4, 0; 0, 0.04]$  meV,  $\delta = 0$  meV,  $\mu = -1$  meV. All other parameters were kept the same.

## Section F: Quantum Liouville evolution and multiband linear and nonlinear response of superconductors.

In this section we systematically derive the photo-response of a multiband superconductor by employing the Hermitian Liouville equation for the Bogoliubov quasiparticles  $i\hbar\partial_t\hat{\rho}(t) = [\hat{H}_{\mathbf{k},\mathbf{q},t}^{\text{BdG}}, \hat{\rho}(t)]$ , where  $\hat{\rho}(t)$  is the time-dependent Bogoliubov quasiparticle density matrix. The most general expansion of the BdG Hamiltonian in powers of electric field can be performed as:

$$\hat{H}_{\mathbf{k},\mathbf{q},t}^{\text{BdG}} = H_{\mathbf{k},\mathbf{q}}^{\text{BdG}} + \frac{e}{\hbar} A_t^\alpha \partial_{\mathbf{q}}^\alpha \hat{H}_{\mathbf{k},\mathbf{q}}^{\text{BdG}} = + \frac{1}{2!} \frac{e^2}{\hbar^2} A_t^\alpha A_t^\beta \partial_{\mathbf{q}}^\alpha \partial_{\mathbf{q}}^\beta \hat{H}_{\mathbf{k},\mathbf{q}}^{\text{BdG}} + \frac{1}{3!} \frac{e^3}{\hbar^3} A_t^\alpha A_t^\beta A_t^\gamma \partial_{\mathbf{q}}^\alpha \partial_{\mathbf{q}}^\beta \partial_{\mathbf{q}}^\gamma \hat{H}_{\mathbf{k},\mathbf{q}}^{\text{BdG}} + \mathcal{O}(E^4). \quad (\text{F-1})$$

Next we aim to clarify the matrix elements in the Bogoliubov basis for each of the terms in Eq. (F-1). We start from the considering the following quantity:

$$\langle \psi_a | (\partial_{\mathbf{q}}^\alpha O) | \psi_b \rangle = \partial_{\mathbf{q}}^\alpha (\langle \psi_a | O | \psi_b \rangle) - \langle \partial_{\mathbf{q}}^\alpha \psi_a | O | \psi_b \rangle - \langle \psi_a | O | \partial_{\mathbf{q}}^\alpha \psi_b \rangle = \partial_{\mathbf{q}}^\alpha O_{ab} - i[A^\alpha, O]_{ab}, \quad (\text{F-2})$$

where we used  $\partial_{\mathbf{q}}^\alpha (\langle \psi_a | \psi_b \rangle) = 0$  and the resolution of identity in the Bogoliubov states so that  $[A, B]_{ab} \equiv \sum_c A_{ac} B_{cb} - B_{ac} A_{cb}$ . Applying this procedure multiple times, we find the following identities:

$$h_{ab}^\alpha = \langle \psi_a | (\partial_{\mathbf{q}}^\alpha H_{\mathbf{k},\mathbf{q}}^{\text{BdG}}) | \psi_b \rangle = \partial_{\mathbf{q}}^\alpha \varepsilon_{\mathbf{k},a}(\mathbf{q}) \delta_{ab} + i[\varepsilon_{\mathbf{k},a}(\mathbf{q}) - \varepsilon_{\mathbf{k},b}(\mathbf{q})] A_{ab}^\alpha, \quad (\text{F-3})$$

$$h_{ab}^{\alpha\gamma} = \langle \psi_a | (\partial_{\mathbf{q}}^\alpha \partial_{\mathbf{q}}^\gamma H_{\mathbf{k},\mathbf{q}}^{\text{BdG}}) | \psi_b \rangle = \partial_{\mathbf{q}}^\alpha h_{ab}^\gamma - i[A^\alpha, h^\gamma]_{ab}, \quad (\text{F-4})$$

$$h_{ab}^{\alpha\beta\gamma} = \langle \psi_a | (\partial_{\mathbf{q}}^\alpha \partial_{\mathbf{q}}^\beta \partial_{\mathbf{q}}^\gamma H_{\mathbf{k},\mathbf{q}}^{\text{BdG}}) | \psi_b \rangle = \partial_{\mathbf{q}}^\beta h_{ab}^{\alpha\gamma} - i[A^\beta, h^{\alpha\gamma}]_{ab}. \quad (\text{F-5})$$

By adopting the adiabatic turning on regularization for the electric field  $E^\alpha(t) = -\partial_t A^\alpha(t) = e^{nt/\hbar} \int_\omega E_\omega^\alpha$  and using the BdG Hamiltonian expansion in Eq.(F-1), we follow the standard perturbation theory and iteratively solve the Liouville equation to find the first order density matrix elements in the Bogoliubov basis as:

$$[\hat{\rho}_1(t)]_{ab} = \int_\omega e^{nt/\hbar} \frac{e}{\hbar} A_\omega^\alpha \frac{h_{ab}^\alpha f_{ba}}{\hbar\omega - \varepsilon_{ab} + i\eta}, \quad (\text{F-6})$$

where  $f_{ab} \equiv f[\varepsilon_{\mathbf{k},a}] - f[\varepsilon_{\mathbf{k},b}]$ ,  $\varepsilon_{ab} \equiv \varepsilon_{\mathbf{k},a}(\mathbf{q}) - \varepsilon_{\mathbf{k},b}(\mathbf{q})$  and the second order as:

$$[\hat{\rho}_2(t)]_{ab} = \iint_{\omega_1\omega_2} \frac{e^{2nt/\hbar} \frac{e}{\hbar} A_{\omega_1}^\alpha \frac{e}{\hbar} A_{\omega_2}^\beta}{\hbar\omega_1 + \hbar\omega_2 - \varepsilon_{ab} + 2i\eta} \left[ \frac{1}{2} h_{ab}^{\alpha\beta} f_{ba} + \sum_c \frac{h_{ac}^\beta h_{cb}^\alpha f_{bc}}{\hbar\omega_1 - \varepsilon_{cb} + i\eta} - \sum_c \frac{h_{ac}^\alpha h_{cb}^\beta f_{ca}}{\hbar\omega_1 - \varepsilon_{ac} + i\eta} \right]. \quad (\text{F-7})$$

Next, the electric current is evaluated as the trace of the electric current operator  $\hat{j}^\alpha = \partial H / \partial A^\alpha$  with the density matrix:  $j^\gamma = \int_{\mathbf{k}} \text{Tr}[\hat{j}^\gamma \hat{\rho}]$ . Keeping terms up to the second order in  $A$  produces:

$$j^\alpha(t) = \frac{e}{\hbar} \text{Tr} \left[ \left( \hat{h}^\alpha + \frac{e^2}{\hbar^2} A^\beta \hat{h}^{\alpha\beta} + \frac{1}{2} \frac{e^3}{\hbar^3} A^\beta A^\gamma \hat{h}^{\alpha\beta\gamma} \right) (\hat{\rho}_0 + \hat{\rho}_1 + \hat{\rho}_2) \right] + \mathcal{O}(E^3). \quad (\text{F-8})$$

Thus we identify the *linear response* as:

$$j_{(1)}^\alpha(t) = \sum_{ab} \frac{e^2}{\hbar^2} \int_\omega e^{nt/\hbar} A_\omega^\beta \frac{h_{ab}^\beta h_{ba}^\alpha f_{ba}}{\hbar\omega - \varepsilon_{ab} + i\eta} + \frac{e^2}{\hbar^2} \sum_a f_a A_t^\beta h_{aa}^{\alpha\beta}. \quad (\text{F-9})$$

Using Eqs.(F-4) and decomposing partial fractions we obtain:

$$[\sigma^{(1)}]_{\omega}^{\alpha\beta} = -i \frac{e^2}{\hbar} \left[ \frac{1}{\hbar\omega + i\eta} \sum_a f_a \partial^\beta h_{aa}^\alpha + \sum_{ab} \frac{h_{ab}^\beta h_{ba}^\alpha f_{ab}}{\hbar\omega - \varepsilon_{ab} + i\eta} \frac{1}{\varepsilon_{ba}} \right], \quad (\text{F-10})$$

while the *non-linear response* is found to have the following four components:

$$j_{(2)}^{\gamma,1}(t) = \frac{e^3}{\hbar^3} \int_{\omega_1, \omega-\omega_1} A_{\omega_1}^\alpha A_{\omega-\omega_1}^\beta \sum_a \frac{1}{2} f_a h_{aa}^{\alpha\beta\gamma}, \quad (\text{F-11})$$

$$j_{(2)}^{\gamma,2}(t) = \frac{e^3}{\hbar^3} \int_{\omega_1, \omega-\omega_1} A_{\omega_1}^\alpha A_{\omega-\omega_1}^\beta \sum_{abc} \frac{h_{cb}^\alpha h_{ac}^\beta h_{ba}^\gamma}{\hbar\omega - \varepsilon_{ab} + 2i\eta} \left[ \frac{f_{bc}}{\hbar\omega_1 - \varepsilon_{cb} + i\eta} + \frac{f_{ac}}{\hbar\omega - \hbar\omega_1 - \varepsilon_{ac} + i\eta} \right], \quad (\text{F-12})$$

$$j_{(2)}^{\gamma,3}(t) = \frac{e^3}{\hbar^3} \int_{\omega_1, \omega-\omega_1} A_{\omega_1}^\alpha A_{\omega-\omega_1}^\beta \sum_{ab} \frac{f_{ba} h_{ab}^\alpha h_{ba}^{\beta\gamma}}{\hbar\omega_1 - \varepsilon_{ab} + i\eta}, \quad (\text{F-13})$$

$$j_{(2)}^{\gamma,4}(t) = \frac{e^3}{\hbar^3} \int_{\omega_1, \omega-\omega_1} A_{\omega_1}^\alpha A_{\omega-\omega_1}^\beta \sum_{ab} \frac{\frac{1}{2} f_{ba} h_{ab}^{\alpha\beta} h_{ba}^\gamma}{\hbar\omega - \varepsilon_{ab} + 2i\eta}, \quad (\text{F-14})$$

which is consistent with Refs.[25, 26]. We note that due to contraction  $\int_{\omega_1} \sum_{\alpha, \beta} A_{\omega_1}^\alpha A_{\omega-\omega_1}^\beta \chi_{\omega_1, \omega-\omega_1}^{\alpha\beta}$ , physically meaningful part of the  $\chi_{\omega_1, \omega-\omega_1}^{\alpha\beta}$  is the one that is symmetric under simultaneous swapping  $\omega_1 \leftrightarrow \omega - \omega_1, \alpha \leftrightarrow \beta$ , as it is the symmetry of  $A_{\omega_1}^\alpha A_{\omega-\omega_1}^\beta$ . Thus, whenever we *symmetrise*  $\chi_{\omega_1, \omega-\omega_1}^{\alpha\beta}$  as:

$$\chi_{\omega_1, \omega-\omega_1}^{\alpha\beta} \rightarrow \frac{1}{2} \chi_{\omega_1, \omega-\omega_1}^{\alpha\beta} + \frac{1}{2} \chi_{\omega-\omega_1, \omega_1}^{\alpha\beta}, \quad (\text{F-15})$$

the physical current is not affected [31].